

# Inference of Number and Location of Purkinje Root Nodes and Ventricular Conduction Properties from Clinical 12-Lead ECGs for Cardiac Digital Twinning

Julia Camps<sup>1</sup>, Zhinuo Jenny Wang<sup>1</sup>, Rafael Sebastian<sup>2</sup>, Xin Zhou<sup>1</sup>, Brodie Lawson<sup>3</sup>, Lucas Arantes Berg<sup>4</sup>, Kevin Burrage<sup>1,3</sup>, Vicente Grau<sup>1</sup>, Rodrigo Weber<sup>4</sup>, Blanca Rodriguez<sup>1</sup>

<sup>1</sup>University of Oxford, Oxford, United Kingdom

<sup>2</sup>University of Valencia, Valencia, Spain

<sup>3</sup>Queensland University of Technology, Brisbane, Australia

<sup>4</sup>Federal University of Juiz de Fora, Juiz de Fora, MG, Brazil

## Abstract

*The Purkinje network plays a determinant role in the electrical activation sequence of the human heart. However, Purkinje properties cannot be clinically measured directly.*

*Recent studies have successfully demonstrated cardiac digital twins without Purkinje networks, using inference methods integrating cardiac magnetic resonance (CMR) imaging and electrocardiogram (ECG) data. A sophisticated strategy to recover a patient's plausible Purkinje structure would enable these cardiac digital twins to augment clinical data and inform Purkinje-based risk stratification.*

*This study presents and evaluates new computational techniques to infer physiological Purkinje terminal (root node) locations and timings and cardiac conduction properties from clinical CMR and ECG using Eikonal simulations. Our extended sequential Monte Carlo approximate Bayesian computation-based inference method shows an improved match in simulated QRS complexes to Q-wave morphologies in clinical 12-lead ECGs with Pearson's correlation coefficients of 0.89.*

## 1. Introduction

A cardiac digital twin [1] is a virtual tool that mechanistically integrates and augments a patient's clinical dataset using physiological knowledge to inform therapeutic and diagnostic decision-making through simulations.

Previous studies demonstrated the power of patient-specific modelling and simulation testing to augment the interpretation of clinical electrocardiogram (ECG) and cardiac magnetic resonance (CMR) data to improve risk

stratification in poorly understood conditions [2,3].

Recent developments have demonstrated the power of inference methods for generating digital twins of the human heart [4,5]. However, neither of these tools comprises the capability of recovering realistic Purkinje network properties, such as the number and location of physiologically timed root nodes and ventricular conduction properties from standard clinical data.

Pro-arrhythmic abnormalities in the heart's Purkinje network [6] cannot be diagnosed from non-invasive clinical data. This study investigates novel computational tools to generate cardiac digital twins to augment clinical data to gain information on people's ventricular activation properties and their Purkinje networks.

We present a novel electrophysiological cardiac digital twin generation pipeline to recover realistic Purkinje root nodes and ventricular conduction properties from CMR and 12-lead ECG data, using an internal knowledge-based representation of the human Purkinje network.

## 2. Methods

First, we sampled the possible root node locations in the endocardium (Figure 1) and used a novel pseudo-Purkinje strategy, based on Cobiveco's universal ventricular coordinates [7], to assign activation 'delay' times to the Purkinje-myocardial junctions, namely, root nodes. These delay times enable later reconstruction of realistic Purkinje trees. The inference method starts by generating a population of parameter sets for conduction speeds and root nodes, which include the physiological delay times. Next, the inference method [4] iteratively samples activation parameter sets and evaluates the Eikonal and pseudo-ECG equations to compute discrepancies to the clinical QRSs until the stopping criteria are fulfilled.

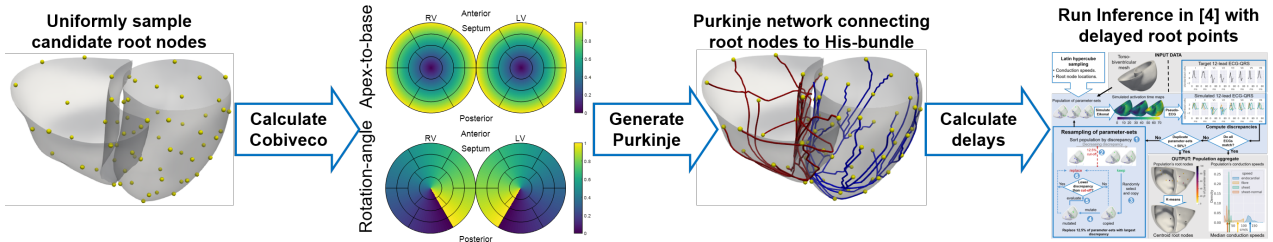


Figure 1. Pseudo-Purkinje generation and inference pipeline. We uniformly sample the root node locations. Then, we generate the Cobiveco coordinates for the endocardial surfaces in both ventricles. Our novel pseudo-Purkinje network algorithm uses them to connect all the candidate root nodes to the His bundle. Next, we compute the root node activation delays. Finally, we run the inference process [4] using these delayed candidate root nodes and the clinical QRS complexes.

## 2.1. Data pre-processing

These clinical ECG recordings were pre-processed by averaging 20 beats and delineating the resulting signals containing the QRS complex [2]. First, we manually segmented the QRS complexes to have a significant gradient at the start of the signals and no gradient at the end. Next, we generated torso-based 12-lead electrode locations and biventricular meshes using the CMR data to enable simulating ECG signals.

## 2.2. Pseudo-Purkinje strategy

We present a strategy based on experimental findings in dogs [8] and humans [9,10] for determining a path between the candidate root nodes in the heart and the his-bundle to pre-compute the root nodes' activation time delays. Our pseudo-Purkinje strategy uses Dijkstra's algorithm to navigate the endocardial cavities from the his-bundle to each root node, passing through different subsets of navigation points depending on where the current root node is located. These navigation points ensure that the his-bundle connects to the different regions in the heart, as observed in experimental data [8-10].

We used the apex-to-base ( $ab$ ) and rotation-angle ( $rt$ ) from the universal ventricular coordinates system Cobiveco [7]. These are symmetric between the right ventricle (RV) and left ventricle (LV) (values from 0 to 1). We define a densely connected, namely 'dense', region of the endocardium that has the most apical ( $ab < 0.4$ ) in the LV and RV, plus the free-wall ( $0.2 < \text{rotation-angle} < 0.5$ ). We refer to the rest of the endocardium as 'sparse'. We define the top and bottom of the his-bundles at the middle of the septal-base line  $[1, 0.85]$  [ $ab, rt$ ] and the most apical-septal point  $[0, 0.85]$ . The root nodes in the RV's free-wall and apical ( $ab < 0.2$ ) regions connect to the point in the non-basal his-bundle ( $ab < 0.8$ ) that has the most similar  $ab$  value. The apical ( $ab < 0.2/0.4, RV/LV$ ) and septal ( $0.7 < rt$ ) root nodes connect to their closest apical ( $ab < 0.2/0.4, RV/LV$ ) his-bundle point. This is also true for the RV paraseptal ( $rt < 0.2 \mid 0.5 < rt < 0.7$ ) root nodes. The LV paraseptal root nodes ( $ab > 0.4 \ \& \ (rt < 0.2 \mid 0.5 < rt < 0.7)$ )

connect to their mid-paraseptal-apical point ( $[0.4, 0.1]$  or  $[0.4, 0.6]$ ) and from there to the closest point in the his-bundle ( $ab < 0.4$ ). The root nodes in the LV's free wall are connected to the his-bundle from the apex to the base. These root nodes connect to the mid-free-wall-apical point ( $[0.4, 0.35]$ ) and then to their closest point in the apical his-bundle ( $0.4 < ab$ ).

This strategy provides a physiological alternative to the simultaneously activated root nodes utilised in previous studies [4,5].

## 2.3. Inference process

We extend our SMC-ABC-based method [4] to infer the human ventricular activation properties and non-simultaneously activated root nodes. We consider the conduction speeds that have a more significant effect on the activation sequence, namely, sheet (i.e. transmural) and fast endocardial speeds, split into dense endocardial speed and sparse endocardial speed to account for the changes in the density of myocardial-Purkinje junctions observed in experimental studies [8,10]. On the other hand, we set the fibre and sheet-normal myocardial conduction speeds to human values, namely, 65 and 48 cm/s [11], respectively. Similarly, we considered a Purkinje speed of 2 m/s [9].

From the resulting population from the inference process, we chose the parameter-set with the highest Pearson's correlation coefficient (PCC) between its simulated 12-lead QRS and the clinical recording.

## 3. Results

Here we present the inference results with simultaneous activation and compare them to the results with our root node delays. We repeated each inference run three times to ensure the reproducibility of our results.

Table 1. Inferred speeds (cm/s) and Pearson's correlation coefficients (PCC) between the recovered and clinical ECGs (mean  $\pm$  standard deviation).

Root node activations	Sheet speed	Sparse speed	Dense speed	Pearson's CC
Simultaneous	29 ±5	83 ±9	124 ±2	0.90 ±0.00
Delayed	39 ±12	120 ±3	111 ±18	0.89 ±0.02

The values inferred for the sheet and sparse-endocardial

speeds were faster when considering Purkinje-driven delays at the root nodes, whereas the dense-endocardial speed was slower. The PCC between the simulated ECG using the inferred activation properties and the clinical QRS signals were equivalent with and without physiological delays at the root nodes.

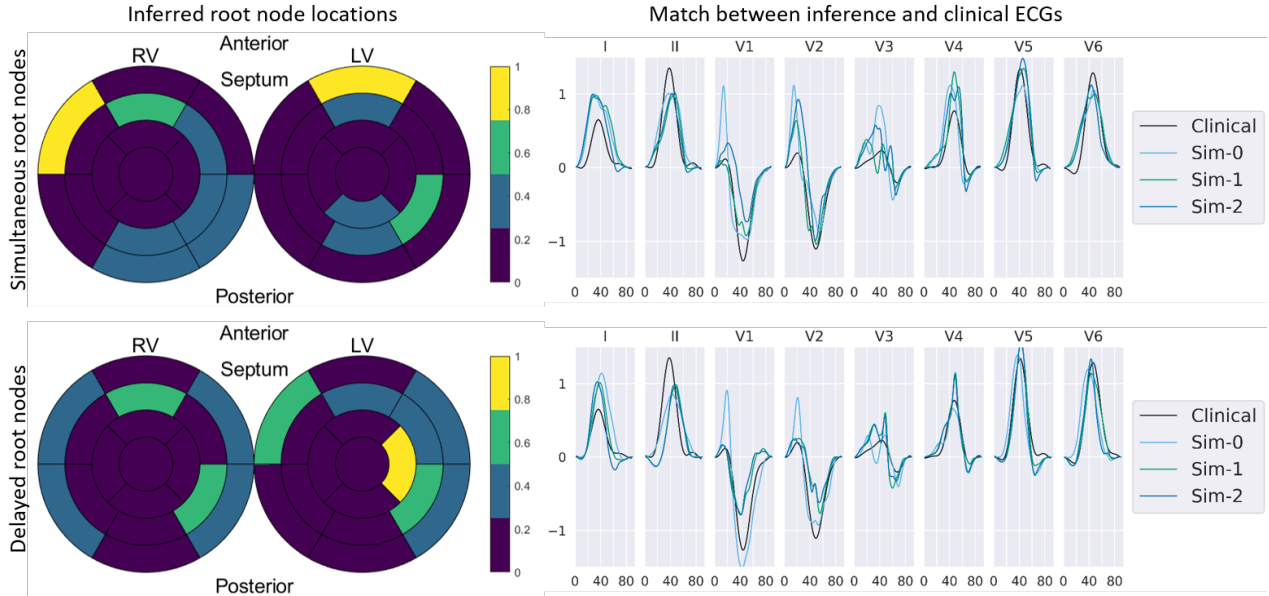


Figure 2. Inferred root node locations (left) and match to the same (top and bottom) clinical ECG (right) using simultaneously activated root nodes (top) and delayed activation at the root nodes from a realistic Purkinje network (bottom). The inferred root nodes obtained from the three runs of the inference process are represented as the frequency of an inference result showing any number of root nodes in each segment of the surface 17-segment (AHA) [12] projections of both ventricles. Yellow indicates that all three runs of the inference had one root node in a region, whereas purple indicates that none of the inference runs returned a root node in that region. The normalised ECG plots show the clinical ECG recording in black and the result of the three runs of the inference in other colours.

For the inference using simultaneously activated root nodes (Figure 2 – top-left), the root nodes were consistently inferred to be located in the basal anterolateral region of the RV and in the basal anterior region of the LV. In the RV, the remaining root nodes were scattered across the mid non-lateral ring and the basal inferior and basal inferoseptal regions. In the LV, these were located in the mid anterior, mid inferior, mid inferoseptal, and apical inferior regions of the endocardial cavity.

The results from the inference using our novel Purkinje-informed delays at the root nodes (Figure 2 – bottom-left) consistently returned root nodes in the apical septal region of the LV. In contrast, in the RV, no region was chosen in all three runs of the inference. The remaining root nodes were scattered across the basal lateral, basal septal, mid anterior and mid inferoseptal regions of the RV and the basal lateral, basal anteroseptal, mid anterior, and mid septal regions of the LV. Overall, we observed a shift towards more lateral inferred locations in the LV when

including the physiological delays at the root nodes.

Regarding the morphological match between the inferred and clinical QRS signals (Figure 2 - right), despite the equivalent PCC scores from both root node activation strategies, including the delays in the root nodes, enabled matching better the small negative deflections present in the Q-waves in leads I, II, V2, V5 and V6 compared to the results from the inference with simultaneously activated root nodes.

#### 4. Discussion

We present a novel digital twin generation pipeline capable of recovering the human ventricular activation properties, including Purkinje structures within human and dog [8-11] experimental ranges, using clinical cine CMR and 12-lead ECG recordings. We demonstrate its application to augment clinical data from one control subject, where we matched the clinical data with PCC of

0.89 between the simulated and clinical QRS complexes. In addition, we showcase the morphological improvement of our extended pipeline in recovering QRS complexes. More precisely, our proposed strategy matches the subject's clinically observed Q-wave morphologies, which was impossible with the previous inference method [4]. These improvements will be key for applying our pipeline to cohorts of subjects presenting pathological Q-waves.

Our method recovers the necessary ingredients for growing complex Purkinje networks in our digital twins of the human ventricular electrophysiology to aid clinicians in Purkinje-related risk stratification by augmenting the information in clinical recordings.

## Acknowledgements

This work was funded by an Engineering and Physical Sciences Research Council doctoral award to Julia Camps, a Wellcome Trust Fellowship in Basic Biomedical Sciences to Blanca Rodriguez (214290/Z/18/Z), the CompBioMed 2 Centre of Excellence in Computational Biomedicine (European Commission Horizon 2020 research and innovation programme, grant agreement No. 823712), the Australian Research Council Centre of Excellence for Mathematical and Statistical Frontiers (CE140100049), and an Australian Research Council Discovery Project (DP200102101). The computation costs were incurred through a PRACE ICEI project (icp013), which provided access to Piz Daint at the Swiss National Supercomputing Centre, Switzerland.

This research was funded in part by the Wellcome Trust [grant number 214290/Z/18/Z]. For the purpose of open access, the author has applied a Creative Commons Attribution (CC BY) public copyright licence to any Author Accepted Manuscript version arising from this submission.

## References

- [1] J. Corral-Acero, F. Margara, M. Marciniak, C. Rodero, F. Loncaric, Y. Feng, A. Gilbert, J.F. Fernandes, H.A. Bukhari, A. Wajdan, M.V. Martinez, M.S. Santos, M. Shamohamdi, H. Luo, P. Westphal, P. Leeson, P. DiAchille, V. Gurev, M. Mayr, L. Geris, P. Pathmanathan, T. Morrison, R. Cornelussen, F. Prinzen, T. Delhaas, A. Doltra, M. Sitges, E.J. Vigmond, E. Zacur, V. Grau, B. Rodriguez, E.W. Remme, S. Niederer, P. Mortier, K. McLeod, M. Potse, E. Pueyo, A. Bueno-Orovio, P. Lamata, "The "Digital Twin" to enable the vision of precision cardiology", *European Heart Journal*, vol. 41, no. 48, pp. 4556-4564, Mar. 2020.
- [2] A. Lyon, A. Bueno-Orovio, E. Zacur, R. Ariga, V. Grau, B. Rodriguez, and A. Mincholé, "Electrocardiogram Phenotypes in Hypertrophic Cardiomyopathy Caused by Distinct Mechanisms: Apico-Basal Repolarization Gradients vs. Purkinje-Myocardial Coupling Abnormalities", *EP Europace*, vol. 20, no. suppl\_3, pp. 102-112, Nov. 2018.
- [3] Z.J. Wang, A. Santiago, X. Zhou, L. Wang, F. Margara, F. Levrero-Florencio, A. Das, C. Kelly, E. Dall'Armellina, M. Vazquez, and B. Rodriguez, "Human biventricular electromechanical simulations on the progression of electrocardiographic and mechanical abnormalities in post-myocardial infarction", *EP Europace*, vol. 23, no. suppl\_1, pp. 143-152, Mar. 2021.
- [4] J. Camps, B. Lawson, C. Drovandi, A. Mincholé, Z.J. Wang, V. Grau, K. Burrage, and B. Rodriguez, "Inference of ventricular activation properties from non-invasive electrocardiography", *MIA*, vol. 73, no. 102143, Oct. 2021.
- [5] K. Gillette, M.A.F. Gsell, A.J. Prassl, E. Karabelas, U. Reiter, G. Reiter, T. Grandits, C. Payer, D. Štern, M. Urschler, J.D. Bayer, C.M. Augustin, A. Neic, T. Pock, E.J. Vigmond, and G. Plank, "A Framework for the generation of digital twins of cardiac electrophysiology from clinical 12-lead ECGs", *MIA*, vol. 71, Jul. 2021.
- [6] M. Haissaguerre, E. Vigmond, B. Stuyvers, M. Hocini, and O. Bernus, "Ventricular Arrhythmias and the His-Purkinje System", *Nat. Rev. Cardiol.*, vol. 13, no. 3, pp. 155-66, Jan. 2016.
- [7] S. Schuler, N. Pilia, D. Potyagaylo, A. Loewe, "Cobiveco: Consistent biventricular coordinates for precise and intuitive description of position in the heart – with MATLAB implementation", *MIA*, vol. 74, no. 102247, Dec. 2021.
- [8] R.J. Myerburg, K. Nilsson, and H. Gelband, "Physiology of Canine Intraventricular Conduction and Endocardial Excitation", *Circ. Res.*, vol. 30, no. 2, pp. 217-243, Feb 1972.
- [9] D. Durrer, R.Th. Van Dam, G.E. Freud, M.J. Janse, F.L. Meijler, and R.C. Arzbaecher, "Total Excitation of the Isolated Human Heart", *Circ.*, vol. 41, no. 6, pp. 899-912, Jun. 1970.
- [10] F. Barber, P. Langfield, M. Lozano, I. Garcia-Fernandez, J. Duchateau, H. Meleze, M. Haissaguerre, E. Vigmond R. Sebastian, "Estimation of personalized minimal Purkinje systems from human electro-anatomical maps", *IEEE Transactions on Medical Imaging*, vol. 40, no. 8, pp. 2182-2194, Apr. 2021.
- [11] P. Taggart, P.M.I. Sutton, T. Opthof, R. Coronel, R. Trimlett, W. Pugsley, and P. Kallis, "Inhomogeneous Transmural Conduction During Early Ischaemia in Patients with Coronary Artery Disease", *JMCC*, vol. 32, no. 4, pp. 621-630, Apr. 2000.
- [12] M.D. Cerqueira, N.J. Weissman, V. Dilsizian, A.K. Jacobs, S. Kaul, W.K. Laskey, D.J. Pennell, J.A. Rumberger, T. Ryan, and M.S. Verani, "Standardized Myocardial Segmentation and Nomenclature for Tomographic Imaging of the Heart", *Circ.*, vol. 105, no. 4, pp. 539-542, Jan. 2002.

Address for correspondence:

Julia Camps.  
Department of Computer Science, University of Oxford,  
Wolfson Building, Parks Road, OXFORD, OX1 3QD, UK.  
julia.camps@cs.ox.ac.uk